MODELLING FOR INFRARED VACUMM DRYING PROCESS

Minh Tuan Hoang[1], Thi Thu Hang Tran[2,*]

DOI: https://doi.org/10.57001/huih5804.2026.136

ABSTRACT

This paper presents the modeling results of the drying process of sliced potatoes in different pressure drying environments, with or without infrared heating. The theoretical model is built based on the volumetric averaging method to establish phase equilibrium within a volume element. Infrared energy is modeled as radiant heat exchange with heat flux density considered as a type 2 boundary condition. The model was solved using MATLAB, and the results were evaluated as highly accurate. The model showed the moisture and temperature distribution in the material throughout the drying process. Calculation results are shown for different pressure and radiation intensity cases to evaluate the effects of drying conditions on drying time. When pressure decreases, the drying rate increases while the material temperature decreases; when radiation intensity increases, the evaporation rate increases but also the material temperature increases

Keywords: *Infrared drying, vacuum drying, small sample, potato, volumetric averaging technique.*

[1]Hue Industrial College, Vietnam
[2]School of Mechanical Engineering, Hanoi University of Science and Technology, Vietnam
[*]Email: hang.tranthithu@hust.edu.vn
Received: 07/3/2026
Revised: 04/5/2026
Accepted: 25/5/2026

NOMENCLATURE

a_w	-	Water activity
c	J/kg.K	Specific heat capacity
D	m^2/s	Diffusivity
h	J/kg	Enthalpy
K	m	Permeability
$\dot{m}$	$Kg/m^3.s$	Volumetric evaporation rate
p	N/m^2	Pressure
q	W/m^2	Heat flux
T	°C	Temperature
X	kg water/kg dry solid	Moisture content

Greek symbols

α	$W/m^2.K$	Heat transfer coefficient
β	m/s	Mass transfer coefficient
δ_{va}	m^2/s	Binary diffusion of air and vapor mixture
ε	-	Volume fraction
λ	W/m.K	Thermal conductivity
ρ	Kg/m^3	Density
ψ	-	Porosity

Subcripts

a	Air
b	Bulk
eff	Effective
eq	Equilibrium
g	Gas
l	Liquid
0	Initial
s	Solid
v	Vapor

1. INTRODUCTION

Drying technology plays a crucial role in post-harvest processing and preservation. It extends shelf life by inhibiting microbial growth, while also reducing storage volume, packaging requirements, and transportation

weight. In the modern world, the increasing demand for high product quality combined with lower energy consumption necessitates the selection of appropriate drying methods. Vacuum drying stands out as an advanced technique that ensures superior quality and is suitable for a wide range of products [1].

Vacuum drying is a process conducted at pressures lower than atmospheric pressure to reduce the evaporation temperature of moisture and increase the vapor pressure gradient between the material and its surroundings, thereby enhancing the driving force of evaporation. While heat conduction via heating plates is commonly used, it is not recommended for heat-sensitive materials as it can degrade appearance and vitamin content. Non-contact drying using microwaves or infrared radiation serves as an effective solution to this issue [2, 3]. Infrared drying has been applied to various types of products due to its advantages of non-contact heating and uniform heat distribution on the surface [4]. Many studies aiming to model vacuum drying processes using radiation have been conducted through both experimental and theoretical approaches.

Empirical models often aim to describe the evaporation rate over time and have been established for several products such as kiwi [5], lemon [6], ginger [7], and seedless grapes [8]. These studies rely primarily on regression methods, where accuracy depends on the number of experiments and measurement errors. Furthermore, their applicability to conditions outside the experimental range is limited, and certain experiments may be unfeasible. Consequently, these results are mainly used for rapid calculation and verification of experimental regimes.

Several theoretical models have been developed to simulate heat and mass transfer within materials. Among them, Luikov's theory has been applied to describe vacuum drying with convective heating, where specific heat and moisture capacity coefficients are determined experimentally [9]. However, the role of convection in a vacuum environment remains a subject of debate. Fick's law has also been applied to yams under microwave heating [11], where moisture transfer is driven by diffusion via the effective moisture diffusion coefficient. Additionally, moisture transport mechanisms have been described using liquid and vapor permeability [12, 13] for non-contact heating. These models currently require systematic research to provide inputs for process optimization studies.

In this paper, a theoretical model based on Whitaker's volume averaging method [13], accounting for the three-phase equilibrium within thin potato slices, will be applied under various pressures and radiation intensities. The model will elucidate the internal heat and mass transfer mechanisms and evaluate the impact of operating conditions on the evaporation process.

2. MATHEMATICAL MODEL

One representative volume element of potato is presented as Figure 1. The mass balance equation for the liquid phase is formulated based on the following principle: the difference between the liquid flow rates entering and leaving the control volume, combined with the amount of liquid evaporated within it, results in the change of liquid density inside that volume [13]. The mass conservation equation for the liquid phase is written as follows:

$$\frac{\partial}{\partial \tau}\left(\rho_l \varepsilon_l\right)+\nabla.\left(\rho_l v_l\right)+\dot{m}_v=0 \quad (1)$$

Unlike the liquid phase, which is considered pure water, the gas phase is a mixture of dry air and water vapor. The transport of vapor consists of two fundamental mechanisms: the bulk movement of the mixture driven by the total gas phase pressure gradient according to Darcy's law, and the diffusion of water vapor caused by the partial pressure of vapor within the dry air-vapor mixture. For water vapor, the mass balance equation is expressed as:

$$\frac{\partial}{\partial \tau}\left(\rho_v \varepsilon_g\right)+\nabla.\left(\rho_v v_g\right)-\nabla.\left(\rho_g D_{eff}\nabla\left(\frac{\rho_v}{\rho_g}\right)\right)-\dot{m}_v=0 \quad (2)$$

In which, ρ_v and ρ_g are the densities of the vapor and vapor and air mixture. D_{eff} (m^2/s) is the effective diffusivity of vapor in the gas and vapor mixture. This effective diffusivity is calculate from volume fraction of liquid phase ε_l, material porosity ψ and binary diffusivity of air and vapor mixture δ_{va}.

$$D_{eff}=\left(1-\frac{\varepsilon_l}{\psi}\right)\psi\delta_{va} \quad (3)$$

The binary diffusivity of air and vapor mixture δ_{va} is calculated from Schirmer's formula:

$$\delta_{va}\left(T_g,P_g\right)=2.26x10^5\left(\frac{T}{T_R}\right)^{1.81}\frac{P_r}{P_g} \quad (4)$$

With T_R = 273K and P_R = 1bar are the reference temperature and pressure respectively. $\nabla\left(\rho_v/\rho_g\right)$ is the

gradient of the mass fraction (the ratio of vapor density to the total density of the dry air-vapor mixture). The volumetric evaporation rate term $\dot{m}_v$ acts as an internal source with a positive value when writing the mass balance for vapor, and as an internal source with a negative value when writing it for liquid water. This is the fundamental difference between the balance equations for liquid water and water vapor. By combining equations (1) and (2), we obtain the mass balance equation for water in both liquid and vapor phases:

$$\frac{\partial}{\partial\tau}\left(\rho_l\varepsilon_l+\rho_v\varepsilon_g\right)+\nabla.\left(\rho_l v_l\right)+\nabla.\left(\rho_v v_g\right)-\nabla.\left(\rho_g D_{eff}\nabla\left(\frac{\rho_v}{\rho_g}\right)\right)=0 \quad (5)$$

Similar to the mass balance equation for water vapor, the mass balance equation for dry air is formulated as follows

$$\frac{\partial}{\partial\tau}\left(\rho_a\varepsilon_g\right)+\nabla.\left(\rho_a v_g\right)-\nabla.\left(\rho_g D_{eff}\nabla\left(\frac{\rho_a}{\rho_g}\right)\right)=0 \quad (6)$$

Considering on a control volume, the difference between the enthalpy fluxes of liquid, vapor, and dry air entering and leaving the volume, combined with the heat flux conducted under the influence of temperature gradients, accounts for the change in internal energy density within that volume:

$$\frac{\partial}{\partial\tau}\left(\rho_s\varepsilon_s h_s+\rho_l\varepsilon_l h_l+\rho_v\varepsilon_g h_v+\rho_a\varepsilon_g h_a\right)+\nabla.\left[\rho_l h_l v_l+\left(\rho_v h_v+\rho_a h_a\right)v_g\right]-\nabla.\left[h_a\rho_g D_{eff}\nabla\left(\frac{\rho_a}{\rho_g}\right)\right]-\nabla.\left[h_v\rho_g D_{eff}\nabla\left(\frac{\rho_v}{\rho_g}\right)\right]-\nabla.\left[\lambda_{eff}\nabla t\right]=0 \quad (7)$$

In the above equation, assuming that the specific heat capacities of the components are constant and temperature-independent, the enthalpies of the solid, liquid, and dry air phases are determined as follows:

$$h_{s/l/a}=c_{p,s/l/a}\left(T-T_R\right) \quad (8)$$

With $c_{p,s/l/a}$ are the heat capacity (J/kg.K) of the solid, liquid, and dry air phases, respectively. The enthalpy of water vapor, specifically, is determined by the following formula:

$$h_v=\Delta h_{evp}\left(T_R+c_{p,v}\right)\left(T-T_R\right)$$

In which, $\Delta h_{evp}\left(T_R\right)=2500kJ/kg$ is laten heat of water at 0°C.

During the infrared drying process, with a heat flux density of q_{bx} and an ambient pressure of $p_{g,b}$ is the sum of the partial pressures of water vapor and dry air:

$$p_v\big|_{x=\pm L}+p_a\big|_{x=\pm L}=p_{g,b} \quad (9)$$

$$j_w.n=-\beta\rho_g\left(d\big|_{x=\pm L}-d_{g,b}\right) \quad (10)$$

$$j_e.n=-\alpha\left(t_{g,b}-t\big|_{x=\pm L}\right)-q_{bx}+\Delta h_{evp}\beta\rho_g\left(d\big|_{x=\pm L}-d_{g,b}\right) \quad (11)$$

With the convective heat and mass transfer coefficients determined using the standard Ranz–Marshall equations, extended for non-spherical materials with the characteristic length is the layer thickness:

$$Nu=2+0.6\mathrm{Re}^{\frac{1}{2}}\mathrm{Pr}^{\frac{1}{3}} \quad (12)$$

$$Sh=2+0.6\mathrm{Re}^{\frac{1}{2}}Sc^{\frac{1}{3}} \quad (13)$$

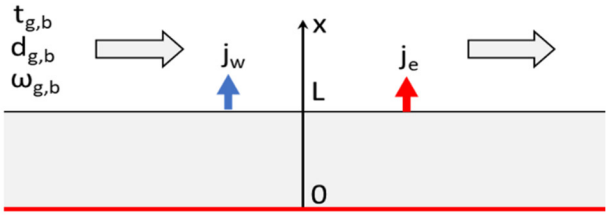

Figure 1. Representative volume of the dried thin layer

Physical properties of potato and air are listed in Table 1 and 2 [15-17].

Table 1. Properties of potato

Properties	Value
Thickness	3 [mm]
Density of solid, ρ_s	1419 [kg/m^3]
Porosity, ψ	0.88
Absolute permeability, K	5×10^{-14} [m^2]
Thermal conductivity of solid	0.21 [W/mK]
Sorption isotherm a_w	$a_w=\frac{\left(X_{eq}/A\right)^{1/B}}{1+\left(X_{eq}/A\right)^{1/B}}$ with A, X_{eq} are taken from [16]

Table 2. Physical properties of air

Properties	Value
Heat capacity of vapor, $c_{p,v}$	2.077 [kJ/kgK]
Heat capacity of water liquid, $c_{p,l}$	4.217 [kJ/kgK]
Heat capacity of air, $c_{p,a}$	1.012 [kJ/kgK]
Density of vapor, ρ_v	$0.598\frac{p_v}{p_{v,s(100^oC)}}.\frac{373.15}{t[^oC]+273.15}$ [kg/m^3]

Density of water liquid, ρ_l	958.35 [kg/m^3]
Density of air, ρ_a	$0.933\frac{p_v}{p_{v,s(100^oC)}}.\frac{373.15}{t[^oC]+273.15}$

The model is implemented using MATLAB version 2025b across various pressure levels and radiation intensities to compare and evaluate the heat and mass transfer processes within the material.

3. RESULTS

3.1. Model validation

To validate the model, experimental results of the dimensionless moisture content of potato slices dried in a GMP 500 commercial dryer will be compared with simulation results under corresponding conditions: an ambient pressure of 1 bar and no radiative heat supply. The potato slices have a thickness of 3 mm, an initial temperature of 20°C, and an initial moisture content of 3.8kg water/kg dry matter. The air velocity is 0.2m/s with a relative humidity of 18%. The dimensionless moisture ratio (MR) is defined as follows:

$$MR = \frac{X - X_{eq}}{X_0 - X_{eq}} \quad (14)$$

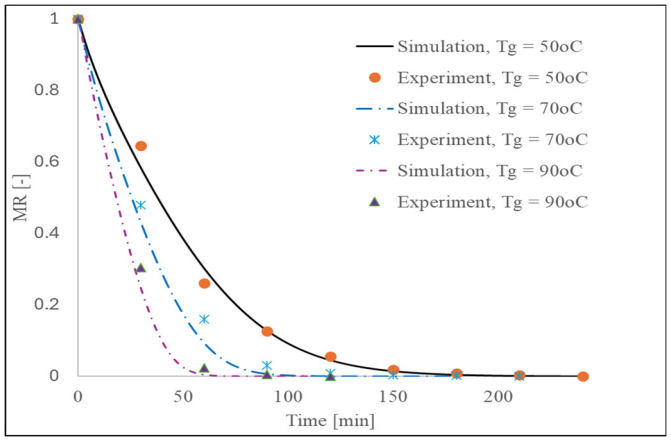

Figure 2. Comparisons of experimental and theoretical results at p = 1bar

It can be observed in Figure 2 that there is good agreement between the exprimental and theoritical data for all gas temperature. Thus, the theoritcal model can be applied for examine the drying kinetic of potato as below section. However, the validation under the vacumm environment drying should be conducted.

3.2. Effects of vacuum drying conditions and radiative heat supply

In this section, simulations were conducted at a gas temperature of T_g = 50°C, with air velocity, pressure, and radiation intensity as listed in Table 3, to evaluate the influence of drying conditions on heat and mass transfer. The simulated results for the average temperature and moisture content of the material across various modes are presented in Figures 3 to 5.

Table 3. Drying modes with varying ambient pressures and radiation intensities

Number of case	Pressure, bar	Infrared intensity, W/m^2
1	1	0
2	0.5	0
3	0.2	0
4	0.1	0
5	1	100
6	0.5	100
7	0.2	100
8	0.1	100
9	1	500
10	0.5	500
11	0.2	500
12	0.1	500

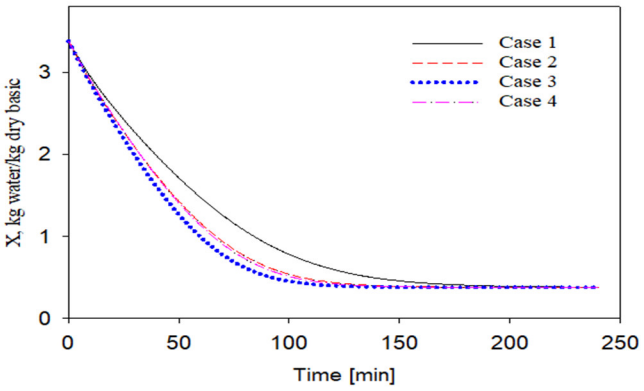

(a)

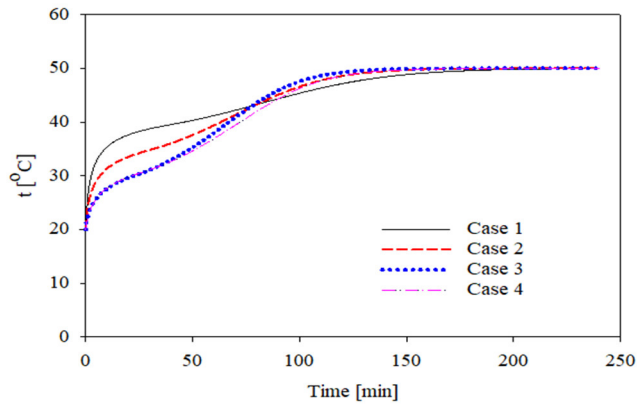

(b)

Figure 3. Simulation results at the heat flux supplied by infrared radiation of q_{bx} = 0W/m^2. (a): Average moisture content; (b): Average temperature

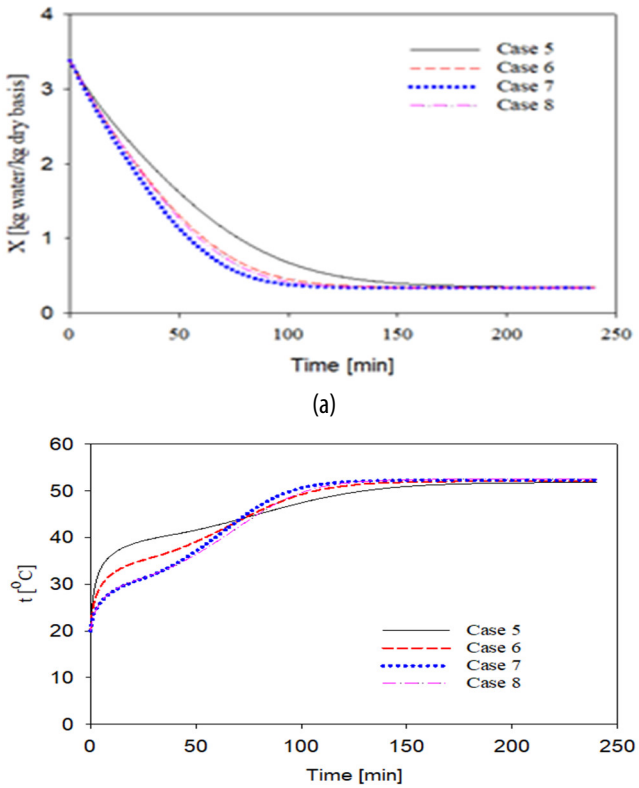

Figure 4. Simulation results at the heat flux supplied by infrared radiation of $q_{bx} = 100W/m^2$. (a): Average moisture content; (b): Average temperature

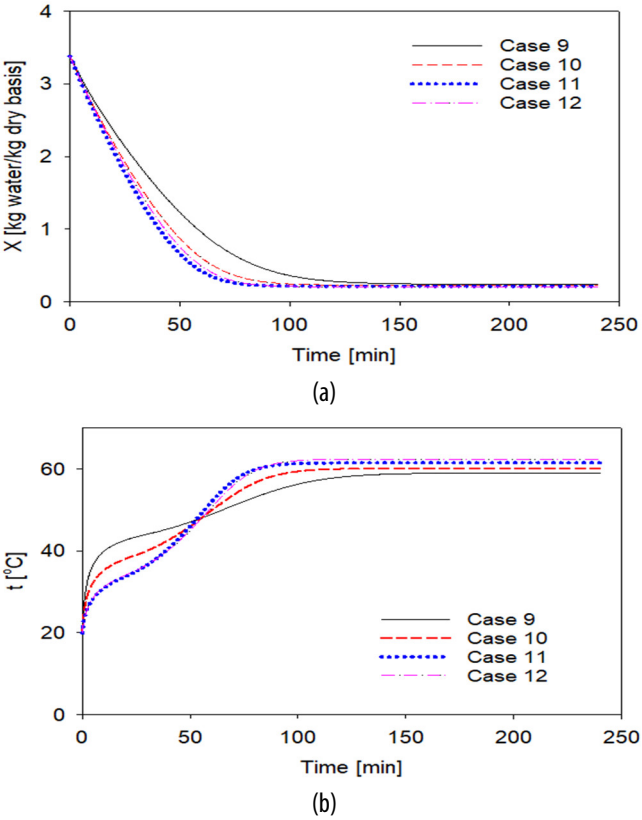

Figure 5. Simulation results at the heat flux supplied by infrared radiation of $q_{bx} = 500W/m^2$. (a): Average moisture content; (b): Average temperature

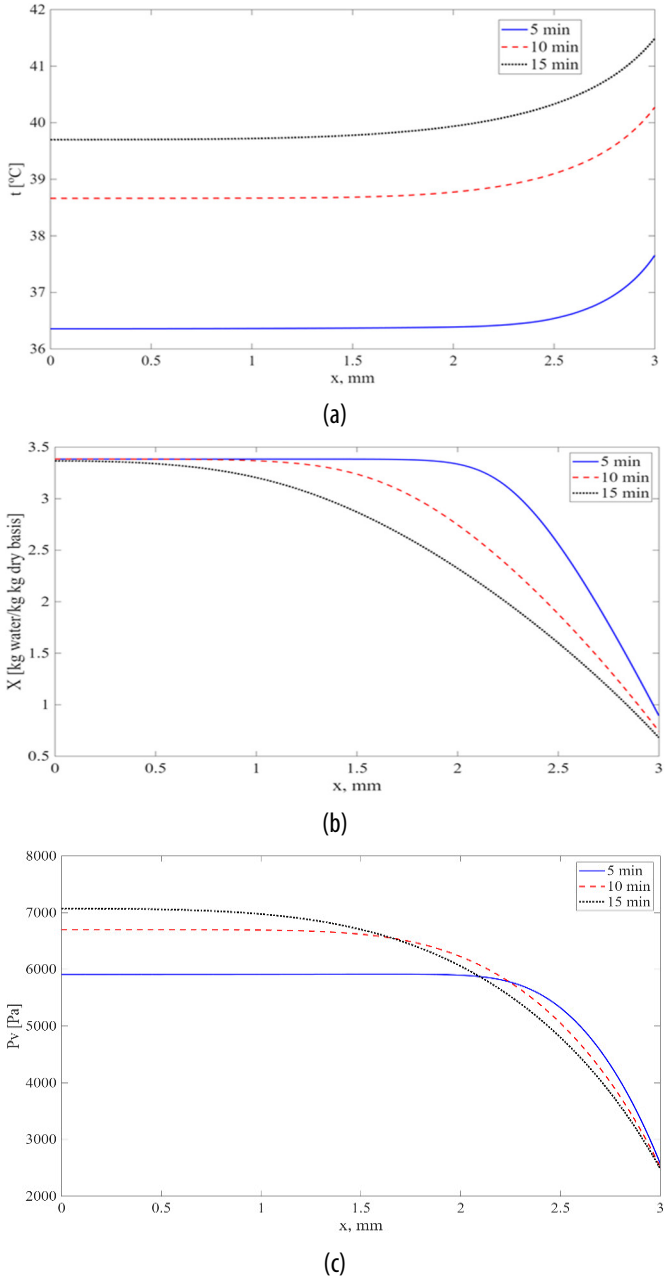

Figure 6. Partial distribution of temperature (a), moisture content (b), vapor pressure (c) with the heat flux supplied by infrared radiation of $q_{bx} = 500W/m^2$ and pressure of 0,2bar

Observing the results under the same radiant heating mode, it is noted that as the ambient pressure decreases, the moisture content of the material slices drops significantly faster compared to that at the ambient pressure in modes 1, 5, and 9. This aligns with theoretical expectations: a reduction in ambient pressure lowers the vapor density in the environment, thereby increasing the driving force for surface evaporation. As the evaporation rate rises, the latent heat required for phase change also increases, leading to a sharp decline in the product temperature. This trend is more pronounced when the

pressure drops significantly from 0.5bar to 0.2bar. However, as the pressure further decreases from 0.2bar to 0.1bar, the evaporation rate only increases during the initial drying stage, causing the material temperature to drop. Subsequently, the evaporation rate plateaus as the material enters a stage where moisture is harder to remove, requiring higher energy; thus, the heat supply becomes the dominant factor affecting evaporation velocity. This pressure reduction helps maintain the material at a lower temperature throughout most of the drying process, which is a key advantage of vacuum drying for controlling product temperature and quality.

Comparing different radiative heat supply modes, the drying process occurs more rapidly. The surface temperature rises faster than in only convective heating. As temperature increases, the vapor pressure at the product surface rises, increasing the surface vapor density and facilitating moisture transport from the surface to the environment. Although radiative heating accelerates the process, it raises the product temperature toward the end of the drying cycle. This suggests that applying controlled radiative heating using high intensity in the initial stage and gradually reducing it toward the end could accelerate drying while effectively managing product temperature.

Figure 6 illustrates the temperature, moisture and vapor pressure distributions of the material at 5, 10, and 15 minutes under a radiation intensity of 500W/m^2 and an ambient pressure of 0.2bar. During the show period, a clear temperature gradient is observed, decreasing from the surface to the base of the sample. Regarding moisture, the outer surface moisture decreases first; after a certain period, the internal moisture begins to drop, with no distinct phase interface. At the later drying time, pressure gradient is steeper because the vapor is generated and comprised more inside the sample. Thus, the theoretical model allows for the investigation of temperature and moisture distribution throughout the drying process.

4. CONCLUSION

This study has developed a theoretical computational model for the drying process of thin-layer materials, which was successfully applied to potatoes. The model is based on the volume averaging method by establishing phase equilibrium equations within the differential element. The simulated drying curves were validated through experimental data, showing high accuracy and confirming the model's reliability. The results indicate that reducing ambient pressure increases the evaporation rate while maintaining a milder material temperature. Conversely, increasing radiative heat flux leads to higher material temperatures toward the end of the drying stage. Furthermore, the model illustrates the internal temperature and moisture distribution, providing insights into the dynamics of evaporation. This work serves as a foundation for future computational fluid dynamic (CFD) modelling research encompassing the entire drying chamber. In the future, the theoretical model should be validated in the vacuum drying system then it can be integrated in the CFD simulation to study drying of the whole drying system to optimize drying conditions in terms of drying time and energy consumption.

SOURCE OF FUNDING

This research was funded by the Ministry of Industry and Trade, Vietnam, under grant number ĐTKHCN.014125.

REFERENCES

[1]. Menon A., Stojceska V., Tassou S. A., "A systematic review on the recent advances of the energy efficiency improvements in non-conventional food drying technologies," *Trends in Food Science & Technology*, 100, 67-76, 2020.

[2]. Liu Z. L., Xie L., Zielinska M., Pan Z., Deng L. Z., Zhang J. S., Gao L., Wang S. Y., Zheng Z. A., Xiao H. W., "Improvement of drying efficiency and quality attributes of blueberries using innovative far-infrared radiation heating assisted pulsed vacuum drying (FIR-PVD)," *Innovative Food Science & Emerging Technologies*, 77, 102948, 2022.

[3]. Li M., Zhu L., Gu J., Li M., Yang X., Zhang Q., "Numerical modelling and experimental study of infrared radiation assisted pulsed vacuum drying of jujube slices," *International Communications in Heat and Mass Transfer,* 168, 109498, 2025.

[4]. Wang J., Law C. L., Nema P. K., Zhao, J. H., Liu Z. L., Deng L. Z., Gao Z. J., Xiao H. W., "Pulsed vacuum drying enhances drying kinetics and quality of lemon slices," *Journal of Food Engineering,* 224, 129-138, 2018.

[5]. Aidani E., Hadadkhodaparast M., Kashaninejad M., "Experimental and modeling investigation of mass transfer during combined infrared-vacuum drying of Hayward kiwifruits," *Food Science Nutrition*, 5, 596-601, 2017.

[6]. Salehi F., Kashaninejad M., "Modeling of moisture loss kinetics and color changes in the surface of lemon slice during the combined infrared-vacuum drying," *Information Processing in Agriculture,* 5(4), 516-523, 2018.

[7]. Wang J., Bai T. Y., Wang D., Fang X. M., Xue L. Y., Zheng Z. A., Gao Z. J., Xiao H. W., "Pulsed vacuum drying of Chinese ginger (Zingiber officinale

Roscoe) slices: Effects on drying characteristics, rehydration ratio, water holding capacity, and microstructure," *Drying Technology,* 37(3), 301-311, 2019.

[8]. Wang J., Xiao H. W., Fang X. M., Mujumdar A. S., Vidyarthi S. K., Xie L., "Effect of high-humidity hot air impingement blanching and pulsed vacuum drying on phytochemicals content, antioxidant capacity, rehydration kinetics and ultrastructure of Thompson seedless grape," *Drying Technology*, 40(5), 1013-1026, 2022.

[9]. Nadi F., Rahimi G. H., Younsi R., Tavakoli T., Hamidi-Esfahani Z., "Numerical Simulation of Vacuum Drying by Luikov's Equations," *Drying Technology*, 30(2), 197-206, 2012.

[10]. Zhang F., Wang X., Xin L., Li L., Dai J., Zhou J., "Moisture diffusion modelling and effect of microwave vacuum drying on drying kinetics and quality of yam," *International Food Research Journal,* 30(3), 626-639, 2023.

[11]. Naderian Jahromi A., Ur Rahman H., Atila Özer M., Ercan O., Ensar Durmuş Ö., Bayraktar S., Lazoglu I., "A novel textile drying technique via pulsed vacuum method," *Drying Technology*, 42(2), 212-226, 2024.

[12]. Salvador A., Teleken J., Travassos X. L., Avila S. L., Carciofi B., "Multiphysics Modeling to Assist Microwave Cavity Design for Food Processing," *International Journal of Electrical and Computer Engineering Research*, 2(2), 1-10, 2022.

[13]. Kharaghani A., Le K. H., Tran T. T. H., Tsotsas E., "Reaction engineering approach for modeling single wood particle drying at elevated air temperature," *Chemical Engineering Science,* 199, 602-612, 2019.

[14]. Vu H. T., Tsotsas E., "Mass and heat transport models for analysis of the drying process in porous media: a review and numerical implementation," *International Journal of Chemical Engineering,* 2018 (3), 1-13, 2018.

[15]. Datta A. K., "Porous media approaches to studying simultaneous heat and mass transfer in food processes. II: Property data and representative results," *Journal of Food Engineering,* 80, 96-100, 2007.

[16]. Addisalem Hailu Taye A. H., Hofacker W. A., Hensel O., "Modeling and the role of water activity, desorption isotherm and glass transition in drying of potatoes quality and shelf life stability," *International Journal of Scientific & Engineering Research*, 12 (12), 352-363, 2021.

[17]. VDI - Gesellshaft energietechnik, *Heat Atlas,* second edition. Springer, Berlin, 2010.